Unusual butane- and pentanetriol-based tetraether lipids in *Methanomassiliicoccus luminyensis*, a representative of the seventh order of methanogens

Running title: Lipid composition of *Methanomassiliicoccus luminyensis*

Kevin W. Becker[a+*], Felix J. Elling[a†], Marcos Y. Yoshinaga[a], Andrea Söllinger[b], Tim Urich[b,§], Kai-Uwe Hinrichs[a]

[a]MARUM Center for Marine Environmental Sciences & Department of Geosciences, University of Bremen, 28359 Bremen, Germany

[b]Department of Ecogenomics and Systems Biology, University of Vienna, 1090 Vienna, Austria

[+]present address: Department of Marine Chemistry and Geochemistry, Woods Hole Oceanographic Institution, Woods Hole, MA 02543, USA.

[†]present address: Department of Earth and Planetary Sciences, Harvard University, Cambridge, MA 02138, USA.

[§]present address: Institute of Microbiology, Ernst Moritz Arndt University Greifswald, 17489 Greifswald, Germany

*Corresponding author: Kevin W. Becker, E-mail: kbecker@whoi.edu

Abstract

A new clade of archaea has recently been proposed to constitute the seventh methanogenic order, the *Methanomassiliicoccales*, which is related to the *Thermoplasmatales* and the uncultivated archaeal clades Deep-Sea Hydrothermal Vent *Euryarchaeota* Group 2 and Marine Group-II *Euryarchaeota*, but only distantly related to other methanogens. In this study, we investigated the membrane lipid composition of *Methanomassiliicoccus luminyensis*, the sole cultured representative of this seventh order. The lipid inventory of *M. luminyensis* comprises a unique assemblage of novel lipids as well as lipids otherwise typical for either thermophilic, methanogenic, or halophilic archaea. For instance, glycerol sesterpanyl-phytanyl diether core lipids mainly found in halophilic archaea were detected, and so were compounds bearing either heptose or methoxylated glycosidic head groups, both of which have so far not been reported for other archaea. The absence of quinones or methanophenazines is consistent with a different biochemistry of methanogenesis compared to the methanophenazine-containing methylotrophic methanogens. The most distinctive characteristic of the membrane lipid composition of *M. luminyensis*, however, is the presence of tetraether lipids in which one glycerol backbone is substituted by either butane- or pentanetriol, i.e., lipids recently discovered in marine sediments. Butanetriol dibiphytanyl glycerol tetraether (BDGT) constitutes the most abundant core lipid type (>50% relative abundance) in *M. luminyensis.* We have thus identified a source for these unusual orphan lipids. The complementary analysis of diverse marine sediment samples showed that BDGTs are widespread in anoxic layers, suggesting an environmental significance of *Methanomassiliicoccales* and/or related BDGT producers beyond gastrointestinal tracts.

Importance

Cellular membranes of members of all three domains of life, *Archaea*, *Bacteria*, and *Eukarya*, are largely formed by lipids in which glycerol serves as backbone for the hydrophobic alkyl chains. Recently, however, archaeal tetraether lipids with either butanetriol or pentanetriol as backbone were identified in marine sediments and attributed to uncultured sediment-dwelling

archaea. Here we show that the butanetriol-based dibiphytanyl tetraethers constitute the major lipids in *Methanomassiliicoccus luminyensis*, the currently only isolate of the novel seventh order of methanogens. Given the absence of these lipids in a large set of archaeal isolates, these compounds may be diagnostic for the *Methanomassiliicoccales* and/or closely related archaea.

Keywords: methanogens; archaea; *Methanomassiliicoccus luminyensis*; membrane lipids; butane- and pentanetriol-based tetraether lipids.

Introduction

Methane is a potent greenhouse gas and an important intermediate in the global carbon cycle (1–3). Biogenic methane is predominantly produced by archaea inhabiting diverse anoxic environments such as sediments, soils, wetlands, and the digestive tracts of termites and ruminants (2, 4). All cultured methanogens to date belong to the phylum *Euryarchaeota*, while metagenomic sequencing revealed a putative methanogenic metabolism for members of the uncultivated *Bathyarchaeota* (formerly known as Miscellaneous Crenarchaeotal Group, MCG) indicating that methanogenesis might not be restricted to the *Euryarchaeota* (5).

Methanogens are classified into seven orders (*Methanobacteriales*, *Methanococcales*, *Methanomicrobiales*, *Methanosarcinales*, *Methanocellales,* *Methanopyrales* and *Methanomassiliicoccales*) that generate methane from H_2/CO_2, acetate, formate, or methylated substrates (2, 6–8). Of these, the *Methanomassiliicoccales* have only recently been described, representing the seventh order of methanogens (6, 7, 9). These *Euryarchaeota* have been detected based on gene biomarker analyses in diverse environments such as lakes, soils, and marine sediments, but are particularly abundant in the digestive tracts of ruminants (10–15). A single pure culture, *Methanomassiliicoccus luminyensis*, as well as a few enrichment cultures have been obtained, all of which reduce methanol or methylamines with H_2 as electron donor (6, 16–20).

The *Methanomassiliicoccales* are only distantly related to other methanogens and form a distinct cluster within the *Thermoplasmata* with the non-methanogenic thermoacidophilic *Thermoplasmatales* and other related lineages such as the Deep-Sea Hydrothermal Vent *Euryarchaeota* Group 2 (DHVEG-2), and the uncultivated Terrestrial Miscellaneous *Euryarchaeota* Group (TMEG), Marine Benthic Group D (MBG-D), and Marine Group II *Euryarchaeota* (MG-II; Fig. 1; 7, 21). Especially the latter two groups are widely distributed in marine sediments and the surface ocean, respectively, but lack cultured representatives (22, 23). Along with the *Methanomassiliicoccales*, MBG-D and other benthic *Euryarchaeota* are of particular interest in environmental microbiology and geosciences as they could be important contributors to microbial biomass and activity in the sedimentary biosphere (24–26). In samples where MBG-D and MG-II dominated 16S rRNA gene libraries, glycerol dibiphytanyl glycerol tetraethers (GDGTs) have frequently been detected as major archaeal lipids, indicating that these archaeal groups may be able to synthesize these lipids (27–29). Moreover, intact GDGTs, e.g., GDGTs attached to glycosidic polar head groups, are commonly used for quantifying archaeal abundance in the subseafloor biosphere (25, 30–33). Understanding the potential sources of GDGTs is of primary importance for reliable quantification of benthic archaeal biomass using lipid biomarkers (31, 32).

Here, we report the lipid composition of the sole isolated representative of the *Methanomassiliicoccales*, *M. luminyensis* strain B10(T). The lipid analyses were facilitated by recently developed HPLC-MS methods that allow the comprehensive, simultaneous analysis of archaeal core and intact polar glycerol-based membrane lipids as well as respiratory quinones, i.e., membrane-bound electron carriers (34, 35). We show that *M. luminyensis* strain B10(T) contains a diverse suite of unique tetraether lipids with either butanetriol or pentanetriol substituting a glycerol backbone moiety. Such lipids were recently found in marine and estuarine sediments, but have not previously been detected in cultured archaeal representatives (36–38). We further documented the distribution of butanetriol-based lipids in diverse marine sediments, which suggested the widespread presence of relatives of *M. luminyensis*.

Material and Methods

Phylogenetic analysis

High quality 16S rRNA gene sequences of archaeal groups of interest (alignment quality >90, pintail 100, sequence quality >90) with a minimum length of 1400 nt were obtained from the SILVA Ref NR SSU r123 database (39). If more than ten sequences per group were downloaded, the sequences were clustered with 94.5% sequence identity using cd-hit-est of the CD-HIT Suite (Huang et al 2010) to obtain representative sequences of different genera (40). After aligning the sequences using the SINA online alignment tool (41) the alignment was improved by gap removal with Gblocks using the least stringent parameters to avoid losing phylogenetic information (42). The alignment was uploaded to the Model Selection tool of the IQ-TREE web server to select the best suited nucleotide substitution model. A maximum likelihood tree was calculated with IQ-TREE applying the GTR model (+F+I+G4) (43). Ultrafast bootstrap (1000 replicates) was used to verify branch support (44). FigTree (http://tree.bio.ed.ac.uk/software/figtree/) and Adobe Illustrator (Adobe Systems Inc., San Jose, CA) were used for visualizing the phylogenetic tree.

Cultivation and lipid extraction

M. luminyensis was grown in an anaerobic medium based on the medium published by Lang et al. (20). Cultures (2 x 20 mL), inoculated with 10% of a previous culture grown under the same conditions, were grown in 120 mL serum flasks at 37 °C for 7 days under an atmosphere containing 80% H_2 and 20% CO_2. Cells were harvested by centrifugation (20 minutes; 13,000 g) and were subsequently lyophilized.

Lipids from *M. luminyensis* were ultrasonically extracted following a modified Bligh & Dyer protocol (45) using a monophasic mixture of methanol, dichloromethane, and aqueous buffer (2:1:0.8, v:v:v). A 50 mM phosphate buffer (pH 7.4) was used for the first two extractions while a 50 mM trichloroacetic acid buffer (pH 2) was used for two additional extractions. The total lipid extracts (TLE) were dried under a stream of N_2 and stored at -20 °C until

measurement. In addition to *M. luminyensis*, twelve marine sediment samples from a variety of depositional environments (Table 2) were analyzed and prepared as described in Liu et al. (31).

Intact polar and core lipid analysis

Intact polar and core lipids were analyzed by injecting TLE aliquots dissolved in methanol:dichloromethane (9:1, v:v) on a Dionex Ultimate 3000 high performance liquid chromatography (HPLC) system connected to a Bruker maXis Ultra-High Resolution quadrupole time-of-flight tandem mass spectrometer equipped with an electrospray ion source operating in positive mode (Bruker Daltonik, Bremen, Germany). The mass spectrometer was set to a resolving power of 27,000 at *m/z* 1,222 and every analysis was mass-calibrated by loop injections of a calibration standard and correction by lock mass, leading to a mass accuracy of better than 1-3 ppm. Ion source and other MS parameters were optimized by infusion of standards (acyclic GDGT (GDGT-0), monoglycosidic (1G-) GDGT-0, diglycosidic (2G-) GDGT-0) into the eluent flow from the LC system using a T-piece.

Analyte separation was achieved using reversed phase (RP) HPLC on an Acquity UPLC BEH C_{18} column (1.7 µm, 2.1 x 150 mm, Waters, Eschborn, Germany) maintained at 65 °C as described by Wörmer et al. (34). The injection volumes was 10 µL and analytes were eluted at a flow rate of 0.4 mL min^{-1} using linear gradients of methanol:water (85:15, v:v, eluent A) to methanol:isopropanol (50:50, v:v, eluent B) both with 0.04% formic acid and 0.1% NH_3. The initial condition was 100% A held for 2 min, followed by a gradient to 15% B in 0.1 min and a gradient to 85% B in 18 min. The column was then washed with 100% B for 8 min.

To determine relative abundances of core lipids, 50% of the TLE was hydrolyzed with 1 M HCl in methanol for 3 h at 70 °C to yield core lipids (46). Additionally, biomass was hydrolyzed directly using 1 M HCl in methanol for 16 h at 70 °C; subsequently lipids were

ultrasonically extracted three times from hydrolyzed biomass using DCM:MeOH 5:1 (v:v). The hydrolyzed TLE and the extract obtained from hydrolyzed biomass were analyzed on the same HPLC-MS system using normal phase (NP) chromatography and an atmospheric pressure chemical ionization-II ion source operated in positive mode, as described by Becker et al. (47). Briefly, hydrolyzed TLE aliquots were dissolved in *n*-hexane:2-propanol (99.5:0.5, v:v) and injected onto two coupled Acquity BEH Amide columns (2.1 x 150 mm, 1.7 µm particle size, Waters, Eschborn, Germany) maintained at 50 °C. The injection volume was 10 µL. Lipids were eluted using linear gradients of *n*-hexane (eluent A) to *n*-hexane:2-propanol (90:10, v:v; eluent B) at a flow rate of 0.5 mL min^{-1}. The initial gradient was 3% B to 5% B in 2 min, followed by increasing B to 10% in 8 min, to 20% in 10 min, to 50% in 15 min and 100% in 10 min, followed by 6 min at 100% B to flush and 9 min at 3% B to re-equilibrate the columns.

Lipids were identified by retention time as well as accurate molecular mass and isotope pattern match of proposed sum formulas in full scan mode and MS^2 fragment spectra. Integration of peaks was performed on extracted ion chromatograms of ±10 mDa width and included the $[M+H]^+$ ions for NP-HPLC-MS and additionally $[M+NH_4]^+$ and $[M+Na]^+$ ions for RP-HPLC-MS. Where applicable, doubly charged ions were included in the integration.

Lipid abundances were corrected for response factors of commercially available as well as purified standards. Purified standards were obtained from extracts of *Archaeoglobus fulgidus* as described in Elling et al. (46). The abundances of monoglycosidic (1G) glycerol dibiphytanyl glycerol tetraethers (GDGTs) and butanetriol dibiphytanyl glycerol tetraethers (BDGTs) were corrected for the response of purified acyclic 1G-GDGT standard, while monoheptose (1Hp)-1G-BDGT was corrected for the response of purified acyclic 2G-GDGT standard due to the structural similarity of the lipids (Fig.1). The abundances of phosphatidylglycerol (PG), 1G-PG-BDGTs and 1Hp-1G-PG-BDGT were corrected for the response of a commercially available 1G-PG-GDGT standard (Matreya LLC, Pleasant Gap, PA, USA). The abundances of 1G- and 2G-archaeols (ARs) were corrected for the response

of respective purified standard, while triglycosidic (3G-) ARs as well as Methoxy-1G (1MeOG) 1G and 1MeOG-2G-ARs were corrected for the response of 2G-AR. PG-AR abundances were corrected for the response of a commercial phosphatidylethanolamine archaeol standard (Avanti Polar Lipids Inc., Alabaster, AL, USA). Due to the lack of appropriate standards, polyprenols were not corrected for their relative response. The abundances of core GDGTs, BDGTs, pentanetriol dibiphytanyl glycerol tetraethers (PDGTs), glycerol dibiphytanol diethers (GDDs) and butanetriol dibiphytanol diethers (BDDs) were corrected for the response factors of purified GDGT-0, while the abundance of core AR was corrected for the response factors of the respective purified standard. The lower limit of detection for lipids was < 1 pg μL^{-1}.

Results

Intact polar and core lipid composition

Eighteen different intact polar lipids (IPLs) with either di- or tetraether core structure and nine different polar head groups were detected in *M. luminyensis*. Head groups include mono-, di and trihexose, methoxy hexose, phosphatidylglycerol, monoheptose and combinations of the different head group types (Fig. 2 and 3). Detected IPLs comprise AR (two C_{20} isoprenoid side chains), GDGT-0, extended (Ext) and diextended (diExt) AR, the latter containing $C_{20\text{-}25}$ and $C_{25\text{-}25}$ isoprenoidal chains, respectively, as core lipid structures. Methoxy hexose and heptose-containing lipids have been tentatively identified by multiple stage mass spectrometry (Fig. 4, Table 1). Moreover, the dominant compounds were identified as IPLs possessing a butanetriol dibiphytanyl glycerol tetraether (BDGT) core (Fig. 5, Table 1). These unusual tetraether lipids are characterized by the replacement of one glycerol moiety with a butanetriol (37) and have not been found in any other cultured archaea to date. Free core lipids were relatively abundant and occurred as AR, GDGT, BDGT, as well as GDD and BDD. Neither GDD nor BDD lipids were detected as IPLs (see Fig. 3). Besides these IPLs and core lipids, we detected saturated and unsaturated C_{45} and C_{50} polyprenols, which

206 contained up to one double bond per isoprenoid unit. Methanophenazines and respiratory
207 quinones were not detected.

208 Di- and tetraether based IPLs with glycosidic head groups account for 49% of the total lipids,
209 Total phosphate-based lipids comprise 33%, while non-polar free core lipids and polyprenols
210 contribute the remaining 18%. The most abundant single lipid in *M. luminyensis* is a PG-
211 BDGT, contributing 20% to the total lipid pool (see Table 1). Phosphatidylglycerol is the
212 dominant single head group representing 25% of total head groups (Fig. 6a) followed by 1G
213 and 1Hp-1G with 14% and 16%, respectively, while other head groups are equally distributed
214 with 8-9%, except for 3G, which showed the lowest relative abundance (3%). The dominant
215 core structure in *M. luminyensis* in the total di- and tetraether lipid pool, including IPLs, is
216 BDGT, accounting for more than 50% (Fig. 6b). The second most abundant core lipid is
217 diExt-AR with 30%, while all other core lipids comprise <10% of total core lipids.

218 Since not all lipids might be solvent-extractable from cells (48, 49), we acid-hydrolyzed the
219 biomass and compared the core lipid distribution with that obtained from the TLE as well as
220 to that obtained from acid hydrolysis of the TLE (Fig. 6b). The relative abundance of BDGTs
221 was substantially higher (up to 82%) in the extracts obtained after acid hydrolysis of the TLE
222 and direct hydrolysis of the biomass compared to the TLE (Fig. 6b). Similarly, the relative
223 abundance of GDGTs increased to almost 20%. Consequently, several lipids showed
224 strongly reduced abundances in the hydrolyzed extracts or were not detectable anymore as
225 in case of the diether lipids Ext- and diExt-AR. While AR showed a similar relative
226 abundance in the hydrolyzed TLE compared to direct analysis of the TLE, its abundance was
227 particularly low in the hydrolyzed biomass extract. As shown by Huguet et al. (49),
228 concentrations of GDGTs were substantially higher (one to two orders of magnitude) in
229 directly hydrolyzed biomass compared to regular lipid extraction protocols for *Nitrosopumilus*
230 *maritimus* biomass. Thus, although we did not generate quantitative information, BDGT and
231 GDGT concentration in the hydrolyzed biomass might be so high that they overwhelm the
232 signal of the diether compounds during mass spectrometry. Interestingly, in the hydrolyzed

extracts, acyclic to dicyclic PDGT and mono- and bicyclic BDGTs were detected; both compound groups were not detectable in the TLE.

Occurrence of BDGTs in the marine environment

To further examine the environmental significance of the unusual BDGTs, we investigated their distribution in 12 marine sediments from diverse settings (Table 2). BDGTs were detected in two-thirds of the samples, including the Peru Margin, Hydrate Ridge, Mediterranean sapropels, Cascadia Margin and Namibia Margin. In these samples, BDGT core lipids accounted for 0.1 and 3.5% of archaeal core tetraethers (GDGTs + BDGTs; Table 2). BDGTs were not detected in sediments from the Equatorial Pacific, Namibia Margin surface sediment and the deep subsurface of the Cascadia Margin.

Discussion

Lipid inventory of M. luminyensis compared to other archaea

The most distinctive characteristics of the membrane lipid composition of *M. luminyensis* are BDGTs and PDGTs which are present as IPLs and free core lipids and have not been reported from other archaea. Thus, these unusual lipids may be diagnostic for members or close relatives of the *Methanomassiliicoccales*. Both, BDGT and PDGT lipids seem to be selectively bound in the acid-hydrolysable fraction, indicated by higher relative abundances in the hydrolyzed biomass compared to the Bligh and Dyer extract (Fig. 6). Potentially, these lipids are preferentially bound to proteins in the membranes and were released by the acid treatment. In bacteria as well as in archaea, membrane proteins have been shown to selectively bind lipids, such as fatty acids, isoprenoids, and different phospho- and glycolipids, influencing the structural and functional integrity of proteins (e.g., 50, 51–53).

However, the biological function as well as the biosynthetic pathway of BDGTs and PDGTs remain unknown. Since the biosynthesis of archaeal membrane lipids typically involves dihydroxyacetone phosphate (DHAP) as an intermediate that is converted to glycerol-1-

phosphate (G1P; 54), a different biosynthetic pathway might be required for butane- and pentanetriol-containing lipids (37). The genomes of *Methanomassiliicoccales* contain genes well known to be involved in archaeal ether lipid biosynthesis, including genes encoding homologues of G1P dehydrogenase, 3-*O*-geranylgeranyl-*sn*-glycerlyl-1-phosphate (GGGP) and digeranylgeranylglyceryl phosphate (DGGGP) synthases, and four enzymes responsible for the activation of the diglyceride, the addition of polar head groups to the glycerol moiety, and the final production of archaeol via the subsequent reduction of the unsaturated isoprenoid chains (20, 21). Only one gene for GGGP synthase, and no second homologue to this gene could be identified that might encode a hypothetical enzyme catalyzing the formation of a GG-butanetriyl-P or GG-pentanetriyl-P intermediate from butanetriol or pentanetriol, respectively, and geranylgeranyl diphosphate (GGPP). Nevertheless, future studies on *Methanomassiliicoccus* BDGT and PDGT biosynthesis might help to elucidate their unresolved biochemistry. Moreover, although the identification of BDGTs and PDGTs based on HPLC-MS as well as degradation experiments by Zhu et al. (37) seems conclusive, the exact structures of these unusual lipids, e.g., the stereochemistry of the butane- and pentanetriol backbone, remain to be fully resolved, e.g., by using NMR-spectroscopy.

M. luminyensis further possesses a unique membrane lipid composition of mixed di- and tetraethers with glycosidic and phosphatidylglycerol head groups, which differs distinctly from all other methanogens and archaea. While Ext-AR as major core lipid in *M. luminyensis* is widespread in halophilic archaea (55–57), it is only present in trace amounts in other methanogens including *Methanosarcina barkeri* (58) and *Methanothermobacter thermautotrophicus* (59). In environmental samples, the detection of Ext-AR has been frequently associated with methane oxidizing archaea (60–62). The diExt-AR that we detected in *M. luminyensis* has so far only been reported in halophiles (63) and as the dominant lipid in the thermophile *Aeropyrum pernix* (64), but not in methanogens. Moreover, heptose-based membrane lipids have not been reported in Archaea, while heptose is a common constituent of polysaccharides in Bacteria (e.g., 65, 66, 67).

Phosphate-bound polyprenols occur widespread in all domains of life and they mainly function as membrane-bound (poly-)saccharide carriers involved in cell wall assembly (68–72). We found abundant phosphate-free polyprenols in *M. luminyensis*, which have previously been detected in the thermophilic methanogen *M. thermautotrophicus* grown under hydrogen-limitation; it was suggested that they may play a role in membrane stabilization (73). Their high relative abundance (14% of total detected lipids, Table 1) in *M. luminyensis* implies an important role of free polyprenols also in this archaeon. However, their distribution among other archaea has not yet been studied and the function of phosphate-free polyprenols in archaeal cells remains elusive.

The unusual membrane lipid composition of *M. luminyensis* is consistent with its phylogenetically distant relationship to other orders of methanogens (9). Additionally, in contrast to the high diversity of respiratory quinones in related members of the *Thermoplasmatales* (35, 74, 75), no quinones were detected in *M. luminyensis*. Similarly, no methanophenazines, respiratory quinone-analogs found in *Methanosarcinales* (35, 76) and *Methanosaeta* (77), were detected in *M. luminyensis.* This finding supports studies of Lang et al. (20) and Söllinger et al. (15) who suggested that the biochemistry of methanogenesis in *Methanomassiliicoccales* may be fundamentally different from that of other, methanophenazine- and cytochrome-containing methylotrophic archaea.

We further validated the potential of BDGTs and PDGTs as biomarkers for *M. luminyensis* by analyzing 25 cultured archaea that we recently analyzed for their respiratory quinone composition (35). These species cover the phyla *Eury-*, *Cren-* and *Thaumarchaeota* and within the *Euryarchaeota* several methanogens as well as the *Methanomassiliicoccales*-related thermoacidophile *Thermoplasma acidophilum*. We did not detect BDGTs or PDGTs in any of these archaea. This indicates a high chemotaxonomic potential of these lipids for *Methanomassiliicoccales*, although we cannot exclude that other, uncultured archaeal lineages also synthesize these lipids. Thus, BDGT biosynthesis might represent another evolutionarily distinct feature of *Methanomassiliicoccales* similar to the unique pathways for

312 methanogenesis and energy conservation (9, 20, 78). Specific membrane lipid adaptation
313 within the *Thermoplasmata* is supported by the fact that for example *Aciduliprofundum*
314 *boonei* belonging to DSHVE-2 contains H-shaped GDGTs (79), while they have not been
315 reported from *Thermoplasmatales* species (80) as well as were not detected in *M.*
316 *luminyensis*. Analysis of the lipid inventory of other cultured representatives of the seventh
317 order of methanogens are, however, required to provide detailed information about the
318 phylogenetic patterns for the biosynthesis of butane- and pentanetriol-based lipids.

319 ***Implications for environmental studies***

320 Butane- and pentanetriol-based tetraether lipids have recently been identified in a number of
321 environmental settings, such as deeply buried marine (37) and shallow estuarine sediments
322 (36). Meador et al. (36) suggested a potential association of BDGTs with the Miscellaneous
323 Crenarchaeotal Group (MCG) due to the positive correlation of BDGT lipids with the relative
324 abundance of MCG 16S rRNA sequences in microbial communities of estuarine sediments
325 from the White Oak River, NC, USA (hereafter WOR). The authors further interpreted the
326 notable ^{13}C-depletion of BDGTs as evidence for BDGT-producers either being autotrophs or
327 heterotrophs feeding on ^{13}C-depleted substrates. While being consistent with the isotopic
328 lines of evidence, our results suggest that the source of BDGTs in WOR sediments might
329 instead be members or relatives of the *Methanomassiliicoccales* (see Fig. 1). In fact,
330 members of the "environmental clade" of *Methanomassiliicoccales* were previously assigned
331 to TMEG (15). Although *Methanomassiliicoccales* were not specifically described in WOR
332 sediments, which is likely due to the low coverage of commonly used primers for
333 *Methanomassiliicoccales*, closely related clades such as MBG-D and TMEG were abundant
334 in these samples (36, 81). Indeed, we evaluated commonly used primers against
335 *Methanomassiliicoccales*, including the one used to sequence archaea from WOR sediments
336 (23, 82) using TestPrime 1.0 and SILVA SSU r126 RefNR dababase (83), and the coverage
337 was only between 0.5% and 56% for zero mismatches. Accordingly, the positive correlation
338 of MCG with BDGTs in the WOR sediments (36) may instead result from the co-occurrence

of MCG and *Methanomassiliicoccales* and/or uncultivated *Thermoplasmata*, such as TMEG and MBG-D, which was observed by operational taxonomic unit network analysis in various marine sediments (84). However, in samples where MBG-D dominate 16S rRNA clone libraries, both BDGTs and PDGTs were not detected, while GDGTs were the most abundant lipids (27). This suggests that members of the MBG-D inhabiting the Pakistan margin sediments are not a major source for BDGT and PDGT lipids and that BDGT synthesis is limited to a subgroup within the *Thermoplasmata*.

The analysis of twelve globally distributed marine sediments from various environmental settings revealed the widespread occurrence of BDGT core lipids (Table 2), implying a large environmental distribution of *Methanomassiliicoccales* and/or relatives that may constitute additional sources. This supports recent metagenomic studies, which showed that besides gut and rumen (6, 13, 14) *Methanomassiliicoccales* also occur ubiquitously in marine and terrestrial anaerobic environments (10, 15, 84, 85). Similarly to WOR, 16S rRNA gene sequences of *Methanomassiliicoccales* were not reported for the investigated sites likely due to a mismatch of commonly used primers against hitherto undetected clades (23), while other uncultured *Thermoplasmatale* were detected (86). In some samples, for instance in the equatorial Pacific, BDGTs were not detected, which is probably related to low TOC concentrations (30) and sulfate reducing conditions (87) at this site. The relative abundance of BDGTs in the 12 samples analyzed in this study (Table 2) is much lower than in the estuarine WOR sediments, where BDGTs accounted for 15% of the total archaeal core lipid pool on average (36). While this data indicates that the conditions in the WOR sediments select for the BDGT-producers, the factors controlling the distribution of the seventh order of methanogens and how they compete with hydrogenotrophic and methylotrophic methanogens, as they require both H_2 and methanol, remains a target for future studies. If future studies confirm the specificity of BDGTs as biomarkers for the seventh order of methanogens, their detection will enrich strategies for investigating these aspects in environmental samples, cultivation experiments, and the gastro-intestinal tracts of humans and ruminant animals (e.g., 14, 17).

Acknowledgements

We thank X.-L. Liu for providing sediment TLE and T.W. Evans for assistance with sample processing. This study was funded by the European Research Council under the European Union's Seventh Framework Programme–''Ideas'' Specific Programme, ERC grant agreement No. 247153 (Advanced Grant DARCLIFE; PI: K.-U.H.) and by the Deutsche Forschungsgemeinschaft through the Gottfried Wilhelm Leibniz Prize awarded to K.-U.H. (Hi 616-14-1) and instrument grant Inst 144/300-1 (LC-qToF system).). A.S. and T.U. were financially supported by a UNI:DOCS fellowship and a short-term travel grant (KWA) of the University of Vienna (Austria).

References

1. **Montzka SA**, **Dlugokencky EJ**, **Butler JH**. 2011. Non-CO_2 greenhouse gases and climate change. Nature **476**:43–50.
2. **Garcia J-L**, **Patel BKC**, **Ollivier B**. 2000. Taxonomic, phylogenetic, and ecological diversity of methanogenic archaea. Anaerobe **6**:205–226.
3. **Cicerone RJ**, **Oremland RS**. 1988. Biogeochemical aspects of atmospheric methane. Global Biogeochem. Cycles **2**:299–327.
4. **Conrad R**. 2009. The global methane cycle: recent advances in understanding the microbial processes involved. Environ. Microbiol. Rep. **1**:285–292.
5. **Evans PN**, **Parks DH**, **Chadwick GL**, **Robbins SJ**, **Orphan VJ**, **Golding SD**, **Tyson GW**. 2015. Methane metabolism in the archaeal phylum Bathyarchaeota revealed by genome-centric metagenomics. Science **350**:434–438.
6. **Paul K**, **Nonoh JO**, **Mikulski L**, **Brune A**. 2012. "*Methanoplasmatales*," *Thermoplasmatales*-related archaea in termite guts and other environments, are the seventh order of methanogens. Appl. Environ. Microbiol. **78**:8245–8253.
7. **Borrel G**, **O'Toole PW**, **Harris HMB**, **Peyret P**, **Brugère J-F**, **Gribaldo S**. 2013. Phylogenomic data support a seventh order of methylotrophic methanogens and provide insights into the evolution of methanogenesis. Genome Biol. Evol. **5**:1769–

1780.

8. **Sakai S**, **Imachi H**, **Hanada S**, **Ohashi A**, **Harada H**, **Kamagata Y**. 2008. *Methanocella paludicola* gen. nov., sp. nov., a methane-producing archaeon, the first isolate of the lineage “Rice Cluster I”, and proposal of the new archaeal order *Methanocellales* ord. nov. Int. J. Syst. Evol. Microbiol.

9. **Borrel G**, **Parisot N**, **Harris HMB**, **Peyretaillade E**, **Gaci N**, **Tottey W**, **Bardot O**, **Raymann K**, **Gribaldo S**, **Peyret P**, **O’Toole PW**, **Brugère J-F**. 2014. Comparative genomics highlights the unique biology of *Methanomassiliicoccales*, a *Thermoplasmatales*-related seventh order of methanogenic archaea that encodes pyrrolysine. BMC Genomics **15**:679.

10. **Lever MA**. 2013. Functional gene surveys from ocean drilling expeditions - a review and perspective. FEMS Microbiol. Ecol. **84**:1–23.

11. **Wright A-DG**, **Toovey AF**, **Pimm CL**. 2006. Molecular identification of methanogenic archaea from sheep in Queensland, Australia reveal more uncultured novel archaea. Anaerobe **12**:134–139.

12. **Wright A-DG**, **Auckland CH**, **Lynn DH**. 2007. Molecular diversity of methanogens in feedlot cattle from Ontario and Prince Edward Island, Canada. Appl. Environ. Microbiol. **73**:4206–4210.

13. **Janssen PH**, **Kirs M**. 2008. Structure of the archaeal community of the rumen. Appl. Environ. Microbiol. **74**:3619–3625.

14. **Poulsen M**, **Schwab C**, **Jensen BB**, **Engberg RM**, **Spang A**, **Canibe N**, **Højberg O**, **Milinovich G**, **Fragner L**, **Schleper C**, **Weckwerth W**, **Lund P**, **Schramm A**, **Urich T**. 2013. Methylotrophic methanogenic *Thermoplasmata* implicated in reduced methane emissions from bovine rumen. Nat. Commun. **4**:1428.

15. **Söllinger A**, **Schwab C**, **Weinmaier T**, **Loy A**, **Tveit AT**, **Schleper C**, **Urich T**. 2015. Phylogenetic and genomic analysis of *Methanomassiliicoccales* in wetlands and animal intestinal tracts reveals clade-specific habitat preferences. FEMS Microbiol. Ecol. **92**.

16. **Iino T**, **Tamaki H**, **Tamazawa S**, **Ueno Y**, **Ohkuma M**, **Suzuki K**, **Igarashi Y**, **Haruta**

S. 2013. *Candidatus* Methanogranum caenicola: a novel methanogen from the anaerobic digested sludge, and proposal of *Methanomassiliicoccaceae* fam. nov. and *Methanomassiliicoccales* ord. nov., for a methanogenic lineage of the class *Thermoplasmata*. Microbes Environ. **28**:244–250.

17. **Dridi B**, **Fardeau ML**, **Ollivier B**, **Raoult D**, **Drancourt M**. 2012. *Methanomassiliicoccus luminyensis* gen. nov., sp. nov., a methanogenic archaeon isolated from human faeces. Int. J. Syst. Evol. Microbiol. **62**:1902–1907.

18. **Borrel G**, **Harris HMB**, **Tottey W**, **Mihajlovski A**, **Parisot N**, **Peyretaillade E**, **Peyret P**, **Gribaldo S**, **O'Toole PW**, **Brugere J-F**. 2012. Genome sequence of "*Candidatus* Methanomethylophilus alvus" Mx1201, a methanogenic archaeon from the human gut belonging to a seventh order of methanogens. J. Bacteriol. **194**:6944–6945.

19. **Borrel G**, **Harris HMB**, **Parisot N**, **Gaci N**, **Tottey W**, **Mihajlovski A**, **Deane J**, **Gribaldo S**, **Bardot O**, **Peyretaillade E**, **Peyret P**, **O'Toole PW**, **Brugere J-F**. 2013. Genome sequence of "*Candidatus* Methanomassiliicoccus intestinalis" Issoire-Mx1, a third *Thermoplasmatales*-related methanogenic archaeon from human feces. Genome Announc. **1**:e00453–13–e00453–13.

20. **Lang K**, **Schuldes J**, **Klingl A**, **Poehlein A**, **Daniel R**, **Brune A**. 2015. New mode of energy metabolism in the seventh order of methanogens as revealed by comparative genome analysis of "*Candidatus* Methanoplasma termitum." Appl. Environ. Microbiol. **81**:1338–1352.

21. **Borrel G**, **Parisot N**, **Harris H**, **Peyretaillade E**, **Gaci N**, **Tottey W**, **Bardot O**, **Raymann K**, **Gribaldo S**, **Peyret P**, **O'Toole P**, **Brugere J-F**. 2014. Comparative genomics highlights the unique biology of *Methanomassiliicoccales*, a *Thermoplasmatales*-related seventh order of methanogenic archaea that encodes pyrrolysine. BMC Genomics **15**:679.

22. **Karner MB**, **DeLong EF**, **Karl DM**. 2001. Archaeal dominance in the mesopelagic zone of the Pacific Ocean. Nature **409**:507–510.

23. **Teske A**, **Sørensen KB**. 2008. Uncultured archaea in deep marine subsurface

sediments: have we caught them all? ISME J. **2**:3–18.

24. **Lloyd KG**, **Schreiber L**, **Petersen DG**, **Kjeldsen KU**, **Lever M a**, **Steen AD**, **Stepanauskas R**, **Richter M**, **Kleindienst S**, **Lenk S**, **Schramm A**, **Jørgensen BB**. 2013. Predominant archaea in marine sediments degrade detrital proteins. Nature **496**:215–218.

25. **Biddle JF**, **Lipp JS**, **Lever MA**, **Lloyd KG**, **Sørensen KB**, **Anderson R**, **Fredricks HF**, **Elvert M**, **Kelly TJ**, **Schrag DP**, **Sogin ML**, **Brenchley JE**, **Teske A**, **House CH**, **Hinrichs K-U**. 2006. Heterotrophic Archaea dominate sedimentary subsurface ecosystems off Peru. Proc. Natl. Acad. Sci. U. S. A. **103**:3846–3851.

26. **Parkes RJ**, **Cragg B**, **Roussel E**, **Webster G**, **Weightman A**, **Sass H**. 2014. A review of prokaryotic populations and processes in sub-seafloor sediments, including biosphere:geosphere interactions. Mar. Geol. **352**:409–425.

27. **Yoshinaga MY**, **Lazar CS**, **Elvert M**, **Lin Y-S**, **Zhu C**, **Heuer VB**, **Teske A**, **Hinrichs K-U**. 2015. Possible roles of uncultured archaea in carbon cycling in methane-seep sediments. Geochim. Cosmochim. Acta **164**:35–52.

28. **Lincoln SA**, **Wai B**, **Eppley JM**, **Church MJ**, **Summons RE**, **DeLong EF**. 2014. Planktonic Euryarchaeota are a significant source of archaeal tetraether lipids in the ocean. Proc. Natl. Acad. Sci. U. S. A. **111**:9858–9863.

29. **Pearson A**, **Ingalls AE**. 2013. Assessing the use of archaeal lipids as marine environmental proxies. Annu. Rev. Earth Planet. Sci. **41**:359–384.

30. **Lipp JS**, **Morono Y**, **Inagaki F**, **Hinrichs K-U**. 2008. Significant contribution of Archaea to extant biomass in marine subsurface sediments. Nature **454**:991–994.

31. **Liu X**, **Lipp JS**, **Hinrichs K-U**. 2011. Distribution of intact and core GDGTs in marine sediments. Org. Geochem. **42**:368–375.

32. **Lipp JS**, **Hinrichs K-U**. 2009. Structural diversity and fate of intact polar lipids in marine sediments. Geochim. Cosmochim. Acta **73**:6816–6833.

33. **Xie S**, **Lipp JS**, **Wegener G**, **Ferdelman TG**, **Hinrichs K-U**. 2013. Turnover of microbial lipids in the deep biosphere and growth of benthic archaeal populations.

478 Proc. Natl. Acad. Sci. U. S. A. **110**:6010–6014.
479 34. **Wörmer L**, **Lipp JS**, **Schröder JM**, **Hinrichs K-U**. 2013. Application of two new LC–
480 ESI–MS methods for improved detection of intact polar lipids (IPLs) in environmental
481 samples. Org. Geochem. **59**:10–21.
482 35. **Elling FJ**, **Becker KW**, **Könneke M**, **Schröder JM**, **Kellermann MY**, **Thomm M**,
483 **Hinrichs K-U**. 2016. Respiratory quinones in Archaea: phylogenetic distribution and
484 application as biomarkers in the marine environment. Environ. Microbiol. **18**:692–707.
485 36. **Meador TB**, **Bowles M**, **Lazar CS**, **Zhu C**, **Teske A**, **Hinrichs K-U**. 2015. The
486 archaeal lipidome in estuarine sediment dominated by members of the Miscellaneous
487 Crenarchaeotal Group. Environ. Microbiol. **17**:2441–2458.
488 37. **Zhu C**, **Meador TB**, **Dummann W**, **Hinrichs K-U**. 2014. Identification of unusual
489 butanetriol dialkyl glycerol tetraether and pentanetriol dialkyl glycerol tetraether lipids in
490 marine sediments. Rapid Commun. Mass Spectrom. **28**:332–338.
491 38. **Knappy CS**, **Yao P**, **Pickering MD**, **Keely BJ**. 2014. Identification of homoglycerol-
492 and dihomoglycerol-containing isoprenoid tetraether lipid cores in aquatic sediments
493 and a soil. Org. Geochem. **76**:146–156.
494 39. **Quast C**, **Pruesse E**, **Yilmaz P**, **Gerken J**, **Schweer T**, **Yarza P**, **Peplies J**, **Glöckner**
495 **FO**. 2013. The SILVA ribosomal RNA gene database project: improved data
496 processing and web-based tools. Nucleic Acids Res. **41**:D590–D596.
497 40. **Yarza P**, **Yilmaz P**, **Pruesse E**, **Glockner FO**, **Ludwig W**, **Schleifer K-H**, **Whitman**
498 **WB**, **Euzeby J**, **Amann R**, **Rossello-Mora R**. 2014. Uniting the classification of
499 cultured and uncultured bacteria and archaea using 16S rRNA gene sequences. Nat
500 Rev Micro **12**:635–645.
501 41. **Pruesse E**, **Peplies J**, **Glöckner FO**. 2012. SINA: Accurate high-throughput multiple
502 sequence alignment of ribosomal RNA genes. Bioinformatics **28**:1823–1829.
503 42. **Castresana J**. 2000. Selection of conserved blocks from multiple alignments for their
504 use in phylogenetic analysis. Mol. Biol. Evol. **17**:540–552.
505 43. **Nguyen L-T**, **Schmidt HA**, **von Haeseler A**, **Minh BQ**. 2014. IQ-TREE: A fast and

effective stochastic algorithm for estimating maximum likelihood phylogenies. Mol. Biol. Evol. .

44. **Minh BQ**, **Nguyen MAT**, **von Haeseler A**. 2013. Ultrafast approximation for phylogenetic bootstrap. Mol. Biol. Evol.

45. **Sturt HF**, **Summons RE**, **Smith K**, **Elvert M**, **Hinrichs K-U**. 2004. Intact polar membrane lipids in prokaryotes and sediments deciphered by high-performance liquid chromatography/electrospray ionization multistage mass spectrometry - new biomarkers for biogeochemistry and microbial ecology. Rapid Commun. Mass Spectrom. **18**:617–628.

46. **Elling FJ**, **Könneke M**, **Lipp JS**, **Becker KW**, **Gagen EJ**, **Hinrichs K-U**. 2014. Effects of growth phase on the membrane lipid composition of the thaumarchaeon *Nitrosopumilus maritimus* and their implications for archaeal lipid distributions in the marine environment. Geochim. Cosmochim. Acta **141**:579–597.

47. **Becker KW**, **Lipp JS**, **Zhu C**, **Liu X-L**, **Hinrichs K-U**. 2013. An improved method for the analysis of archaeal and bacterial ether core lipids. Org. Geochem. **61**:34–44.

48. **Nishihara M**, **Koga Y**. 1987. Extraction and composition of polar lipids from the archaebacterium, *Methanobacterium thermoautotrophicum*: effective extraction of tetraether lipids by an acidified solvent. J. Biochem. **101**:997–1005.

49. **Huguet C**, **Martens-Habbena W**, **Urakawa H**, **Stahl DA**, **Ingalls AE**. 2010. Comparison of extraction methods for quantitative analysis of core and intact polar glycerol dialkyl glycerol tetraethers (GDGTs) in environmental samples. Limnol. Oceanogr. Methods **8**:127–145.

50. **Laganowsky A**, **Reading E**, **Allison TM**, **Ulmschneider MB**, **Degiacomi MT**, **Baldwin AJ**, **Robinson C V**. 2014. Membrane proteins bind lipids selectively to modulate their structure and function. Nature **510**:172–175.

51. **Yeagle PL**. 2014. Non-covalent binding of membrane lipids to membrane proteins. Biochim. Biophys. Acta - Biomembr. **1838**:1548–1559.

52. **Lee AG**. 2004. How lipids affect the activities of integral membrane proteins. Biochim.

Biophys. Acta - Biomembr. **1666**:62–87.

53. **Eichler J**, **Adams MWW**. 2005. Posttranslational Protein Modification in Archaea. Microbiol. Mol. Biol. Rev. **69**:393–425.

54. **Nishihara M**, **Koga Y**. 1995. *sn*-glycerol-l-phosphate dehydrogenase in *Methanobacterium thermoautotrophicus*: key enzyme in biosynthesis of the enantiomeric glycerophosphate backbone of ether phospholipids of Archaebacteria. J. Biochem. **117**:933–935.

55. **De Rosa M**, **Gambacorta A**, **Nicolaus B**, **Ross HNM**, **Grant WD**, **Bu'Lock JD**. 1982. An asymmetric archaebacterial diether lipid from alkaliphilic halophiles. Microbiology **128**:343–348.

56. **Kates M**. 1996. Structural analysis of phospholipids and glycolipids in extremely halophilic archaebacteria. J. Microbiol. Methods **25**:113–128.

57. **Kates M**. 1993. Biology of halophilic bacteria, Part II − Membrane lipids of extreme halophiles: biosynthesis, function and evolutionary significance, p. 1027–1036. *In* Kushner, MKDJ, Matheson, AT (eds.), The Biochemistry of Archaea (Archaebacteria). Elsevier Science, Amsterdam, The Netherlands.

58. **De Rosa M**, **Gambacorta A**, **Lanzotti V**, **Trincone A**, **Harris JE**, **Grant WD**, **Rosa M De**, **Gambacorta A**, **Lanzotti V**, **Trincone A**, **Harris JE**, **Grant WD**. 1986. A range of ether core lipids from the methanogenic archaebacterium *Methanosarcina barkeri*. Biochim. Biophys. Acta **875**:487–492.

59. **Mancuso CA**, **Odham G**, **Westerdahl G**, **Reeve JN**, **White DC**. 1985. C_{15}, C_{20}, and C_{25} isoprenoid homologues in glycerol diether phospholipids of methanogenic archaebacteria. J. Lipid Res. **26**:1120–1125.

60. **Yoshinaga MY**, **Wörmer L**, **Elvert M**, **Hinrichs K-U**. 2012. Novel cardiolipins from uncultured methane-metabolizing archaea. Archaea **2012**:832097.

61. **Stadnitskaia A**, **Bouloubassi I**, **Elvert M**, **Hinrichs K-U**, **Sinninghe Damsté JS**. 2008. Extended hydroxyarchaeol, a novel lipid biomarker for anaerobic methanotrophy in cold seepage habitats. Org. Geochem. **39**:1007–1014.

562 62. **Yoshinaga MY**, **Kellermann MY**, **Rossel PE**, **Schubotz F**, **Lipp JS**, **Hinrichs K-U**.
563 2011. Systematic fragmentation patterns of archaeal intact polar lipids by high-
564 performance liquid chromatography/electrospray ionization ion-trap mass spectrometry.
565 Rapid Commun. Mass Spectrom. **25**:3563–3574.
566 63. **De Rosa M**, **Gambacorta A**, **Nicolaus B**, **Grant WD**. 1983. A C_{25}, C_{25} diether core
567 lipid from archaebacterial haloalkaliphiles. Microbiology **129**:2333–2337.
568 64. **Morii H**, **Yagi H**, **Akutsu H**, **Nomura N**, **Sako Y**, **Koga Y**. 1999. A novel
569 phosphoglycolipid archaetidyl(glucosyl)inositol with two sesterterpanyl chains from the
570 aerobic hyperthermophilic archaeon *Aeropyrum pernix* K1. Biochim. Biophys. Acta
571 **1436**:426–436.
572 65. **Mayberry WR**, **Smith PF**, **Langworthy TA**. 1974. Heptose-containing pentaglycosyl
573 diglyceride among the lipids of *Acholeplasma modicum*. J. Bacteriol. **118**:898–904.
574 66. **Adams GA**, **Young R**. 1965. Capsular polysaccharides of *Serratia marcescens*. Can.
575 J. Biochem. **43**:1499–1512.
576 67. **Osborn MJ**. 1963. Studies in the Gram-negative cell wall. I. Evidence for the role of 2-
577 keto-3-deoxyoctonoate in the lipopolysaccharide of *Salmonella typhimurium*. Proc.
578 Natl. Acad. Sci. U. S. A. **50**:499–506.
579 68. **Surmacz L**, **Swiezewska E**. 2011. Polyisoprenoids – Secondary metabolites or
580 physiologically important superlipids? Biochem. Biophys. Res. Commun. **407**:627–632.
581 69. **Swiezewska E**, **Danikiewicz W**. 2005. Polyisoprenoids: Structure, biosynthesis and
582 function. Prog. Lipid Res. **44**:235–258.
583 70. **Hartley MD**, **Imperiali B**. 2012. At the membrane frontier: A prospectus on the
584 remarkable evolutionary conservation of polyprenols and polyprenyl-phosphates. Arch.
585 Biochem. Biophys. **517**:83–97.
586 71. **Albers S-V**, **Meyer BH**. 2011. The archaeal cell envelope. Nat. Rev. Microbiol. **9**:414–
587 426.
588 72. **Meyer BH**, **Albers S-V**. 2001. Archaeal Cell Walls. eLS. John Wiley & Sons, Ltd.
589 73. **Yoshinaga MY**, **Gagen EJ**, **Wörmer L**, **Broda NK**, **Meador TB**, **Wendt J**, **Thomm M**,

Hinrichs K-U. 2015. *Methanothermobacter thermautotrophicus* modulates its membrane lipids in response to hydrogen and nutrient availability. Front. Microbiol. **6**:1–9.

74. **Shimada H**, **Shida Y**, **Nemoto N**, **Oshima T**, **Yamagishi A**. 2001. Quinone profiles of *Thermoplasma acidophilum* HO-62. J. Bacteriol. **183**:1462–1465.

75. **Golyshina O V**, **Lünsdorf H**, **Kublanov I V**, **Goldenstein NI**, **Hinrichs K-U**, **Golyshin PN**. 2016. The novel extremely acidophilic, cell-wall-deficient archaeon *Cuniculiplasma divulgatum* gen. nov., sp. nov. represents a new family, *Cuniculiplasmataceae* fam. nov., of the order *Thermoplasmatales*. Int. J. Syst. Evol. Microbiol. **66**:332–340.

76. **Abken HJ**, **Tietze M**, **Brodersen J**, **Bäumer S**, **Beifuss U**, **Deppenmeier U**. 1998. Isolation and characterization of methanophenazine and function of phenazines in membrane-bound electron transport of *Methanosarcina mazei* Gö1. J. Bacteriol. **180**:2027–2032.

77. **Welte C**, **Deppenmeier U**. 2011. Membrane-bound electron transport in *Methanosaeta thermophila*. J. Bacteriol. **193**:2868–2870.

78. **Borrel G**, **Gaci N**, **Peyret P**, **O'Toole PW**, **Gribaldo S**, **Brugere J-F**. 2014. Unique characteristics of the pyrrolysine system in the 7th order of methanogens: implications for the evolution of a genetic code expansion cassette. Archaea **2014**:374146.

79. **Schouten S**, **Baas M**, **Hopmans EC**, **Reysenbach A-L**, **Damsté JSS**. 2008. Tetraether membrane lipids of Candidatus "Aciduliprofundum boonei", a cultivated obligate thermoacidophilic euryarchaeote from deep-sea hydrothermal vents. Extremophiles **12**:119–24.

80. **Shimada H**, **Nemoto N**, **Shida Y**, **Oshima T**, **Yamagishi A**. 2002. Complete Polar Lipid Composition of *Thermoplasma acidophilum* HO-62 Determined by High-Performance Liquid Chromatography with Evaporative Light-Scattering Detection. J. Bacteriol. **184**:556–563.

81. **Lazar CS**, **Biddle JF**, **Meador TB**, **Blair N**, **Hinrichs K-U**, **Teske AP**. 2015. Environmental controls on intragroup diversity of the uncultured benthic archaea of the

618 Miscellaneous Crenarchaeotal Group lineage naturally enriched in anoxic sediments of
619 the White Oak River estuary (North Carolina, USA).
620 82. **Lazar CS**, **Biddle JF**, **Meador TB**, **Blair N**, **Hinrichs K-U**, **Teske AP**. 2014.
621 Environmental controls on intragroup diversity of the uncultured benthic archaea of the
622 Miscellaneous Crenarchaeotal Group lineage naturally enriched in anoxic sediments of
623 the White Oak River Estuary (North Carolina, USA). Environ. Microbiol. **49**.
624 83. **Klindworth A**, **Pruesse E**, **Schweer T**, **Peplies J**, **Quast C**, **Horn M**, **Glöckner FO**.
625 2013. Evaluation of general 16S ribosomal RNA gene PCR primers for classical and
626 next-generation sequencing-based diversity studies. Nucleic Acids Res. **41**:e1–e1.
627 84. **Fillol M**, **Auguet J-C**, **Casamayor EO**, **Borrego CM**. 2015. Insights in the ecology and
628 evolutionary history of the Miscellaneous Crenarchaeotic Group lineage. ISME J.
629 85. **Zhou Z**, **Chen J**, **Cao H**, **Han P**, **Gu J-D**. 2014. Analysis of methane-producing and
630 metabolizing archaeal and bacterial communities in sediments of the northern South
631 China Sea and coastal Mai Po Nature Reserve revealed by PCR amplification of mcrA
632 and pmoA genes. Front. Microbiol. **5**:789.
633 86. **Durbin AM**, **Teske A**. 2012. Archaea in organic-lean and organic-rich marine
634 subsurface sediments: an environmental gradient reflected in distinct phylogenetic
635 lineages. Front. Microbiol. **3**:168.
636 87. **D'Hondt S**, **Jørgensen BB**, **Miller DJ**, **Batzke A**, **Blake R**, **Cragg BA**, **Cypionka H**,
637 **Dickens GR**, **Ferdelman T**, **Hinrichs K-U**, **Holm NG**, **Mitterer R**, **Spivack A**, **Wang**
638 **G**, **Bekins B**, **Engelen B**, **Ford K**, **Gettemy G**, **Rutherford SD**, **Sass H**, **Skilbeck CG**,
639 **Aiello IW**, **Guèrin G**, **House CH**, **Inagaki F**, **Meister P**, **Naehr T**, **Niitsuma S**, **Parkes**
640 **RJ**, **Schippers A**, **Smith DC**, **Teske A**, **Wiegel J**, **Padilla CN**, **Acosta JLS**. 2004.
641 Distributions of microbial activities in deep subseafloor sediments. Science **306**:2216–
642 2221.
643 88. **Liu X-L**, **Summons RE**, **Hinrichs K-U**. 2012. Extending the known range of glycerol
644 ether lipids in the environment: structural assignments based on tandem mass spectral
645 fragmentation patterns. Rapid Commun. Mass Spectrom. **26**:2295–2302.

89. **Elling FJ**, **Könneke M**, **Lipp JS**, **Becker KW**, **Gagen EJ**, **Hinrichs K-U**. 2014. Effects of growth phase on the membrane lipid composition of the thaumarchaeon Nitrosopumilus maritimus and their implications for archaeal lipid distributions in the marine environment. Geochim. Cosmochim. Acta **141**:579–597.

90. **Schouten S**, **Hopmans EC**, **Baas M**, **Boumann H**, **Standfest S**, **Könneke M**, **Stahl DA**, **Sinninghe Damsté JS**. 2008. Intact Membrane Lipids of "Candidatus Nitrosopumilus maritimus," a Cultivated Representative of the Cosmopolitan Mesophilic Group I Crenarchaeota. Appl. Environ. Microbiol. **74**:2433–2440.

91. **Koga Y**, **Morii H**. 2005. Recent advances in structural research on ether lipids from archaea including comparative and physiological aspects. Biosci. Biotechnol. Biochem. **69**:2019–2034.

92. **Knappy CS**, **Nunn CEM**, **Morgan HW**, **Keely BJ**. 2011. The major lipid cores of the archaeon Ignisphaera aggregans: implications for the phylogeny and biosynthesis of glycerol monoalkyl glycerol tetraether isoprenoid lipids. Extremophiles **15**:517–528.

93. **Nichols PD**, **Franzmann PD**. 1992. Unsaturated diether phospholipids in the Antartic methanogen *Methanococcoides burtonii*. FEMS Microbiol. Lett. **98**:205–208.

94. **Wegener G**, **Krukenberg V**, **Ruff SE**, **Kellermann MY**, **Knittel K**. 2016. Metabolic capabilities of microorganisms involved in and associated with the anaerobic oxidation of methane. Front. Microbiol. **7**:46.

95. **Kellermann MY**, **Yoshinaga MY**, **Wegener G**, **Krukenberg V**, **Hinrichs K-U**. 2016. Tracing the production and fate of individual archaeal intact polar lipids using stable isotope probing. Org. Geochem. **95**:13–20.

96. **Pitcher A**, **Rychlik N**, **Hopmans EC**, **Spieck E**, **Rijpstra WIC**, **Ossebaar J**, **Schouten S**, **Wagner M**, **Sinninghe Damsté JS**. 2010. Crenarchaeol dominates the membrane lipids of *Candidatus* Nitrososphaera gargensis, a thermophilic group I.1b Archaeon. ISME J. **4**:542–552.

672 **Table and Figure legends**

673 **Table 1.** IPLs and core lipids in the TLE of M. luminyensis. Molecular masses of $[M+H]^+$,
674 $[M+NH_4]^+$ and $[M+Na]^+$ adducts in positive ion mode RP-HPLC-MS^1, diagnostic fragment ions
675 in MS^2 experiments and relative abundance of lipids are shown. For interpretations of mass
676 spectra see main text. Abbreviations: AR, glycerol diphytanyl diether (archaeol); Ext-AR,
677 glycerol sesterpanyl-phytanyl diether (extended archaeol); diExt-AR, glycerol disesterpanyl
678 diether (diextended archaeol); GDGT, glycerol dibiphytanyl glycerol tetraether; GDD, glycerol
679 dibiphytanol diether; BDGT, butanetriol dibiphytanyl glycerol tetraether; BDD, butanetriol
680 dibiphytanol diether; 1G, monoglycosyl; 2G, diglycosyl; 3G, triglycosyl; 1Hp, monoheptose;
681 PG, phosphatidylglycerol; 1MeOG, methoxyglycosyl.

682 **Table 2.** Percentage of core BDGTs relative to total isoprenoidal core tetraethers
683 [BDGTs/(BDGTs + GDGTs) x 100] in selected sediment samples (n.d., not detected).
684 Detailed information on sampling sites has been published in Liu et al. (31, 88).

685 **Fig. 1.** Phylogenetic tree of archaea, including methanogens and clades found in marine
686 sediments, and the major core lipids described for cultivated and enriched representatives.
687 Lipid data of *Methanomassiliicoccales* from this study, for other cultivated archaea from 27,
688 79, 89–93 and for ANME enrichments from 94, 95. The maximum likelihood tree is derived
689 from nearly full-length 16S rRNA gene sequences. Bootstrap values (1000 replicates) were
690 calculated to verify branch support (● ≥ 95 %; ○ >80%). The scale bar indicates substitutions
691 per site. Abbreviations: MG-II, Marine Group II, DHVEG-2, Deep-Sea Hydrothermal Vent
692 *Euryarchaeota* Group 2; TMEG, Terrestrial Miscellaneous *Euryarchaeota* Group; MBG,
693 Marine Benthic Group; MG, Marine Group; ANME, anaerobic methanotroph; MCG,
694 Miscellaneous Crenarchaeotal Group; GDGT, glycerol dibiphytanyl glycerol tetraether;
695 GTGT, glycerol trialkyl glycerol tetraether; GDD, glycerol dibiphytanyl diether; BDD,
696 butanetriol dibiphytanyl diether; BDGT, butanetriol dibiphytanyl glycerol tetraether; PDGT,
697 pentanetriol dibiphytanyl glycerol tetraether; Uns, unsaturated; Ext, extended, OH, hydroxy;
698 M, macrocyclic; MeO, methoxy; Me, methylated; H, H-shaped.

699 **Fig. 2.** Molecular structures of all identified intact polar and core lipids in
700 *Methanomassiliicoccus luminyensis*. Lipids include glycerol diphytanyl diether (archaeol),
701 glycerol sesterpanyl-phytanyl diether (extended archaeol), glycerol disesterpanyl diether
702 (diextended archaeol), glycerol dibiphytanyl glycerol tetraether (GDGT), glycerol dibiphytanol
703 diether (GDD), butanetriol dibiphytanyl glycerol tetraether (BDGT), butanetriol dibiphytanol
704 diether (BDD), pentanetriol dibiphytanyl glycerol tetraether (PDGT) core lipids and saturated
705 and unsaturated C_{45} and C_{50} polyprenols with up to one double bond per isoprenoid unit.
706 BDGT and PDGT core lipids with one and two cyclopentyl moieties are also shown. Intact
707 polar lipids consist of di- and tetraether core lipids attached to a polar head group.

708 **Fig. 3.** Reversed phase HPLC-MS analyses of *M. luminyensis* TLE showing (a) extracted ion
709 chromatogram of all identified lipids (including C_{46}-GTGT injection standard) and (b) density
710 map plot allowing three-dimensional view on chromatographic separation and mass-to-
711 charge ratio (*m/z*) with intensity on the z-axis (from low intensities indicated by white colors to
712 intermediate intensities indicated by blue color and high intensities indicated by red color).
713 Lipid nomenclature designates combinations of core lipid types (AR, archaeol; Ext-AR,
714 extended-AR; diExt-AR, diextended-AR; GDGT, glycerol dibiphytanyl glycerol tetraether;
715 GDD, glycerol dialkanol diether; BDGT, butanetriol dibiphytanyl glycerol tetraether; BDD,
716 butanetriol dibiphytanol diether) and head groups (PG, phosphatidylglycerol; 1G,
717 monoglycosyl; 2G, diglycosyl; 3G, triglycosyl; PG, phosphatidyl glycerol; 1Hp-1G,
718 monoheptose-1G; 1G-PG; 1Hp-1G-PG; 1MeOG-1G, methoxy-1G; 1MeOG-2G). For
719 structures of lipids see Fig. 2.

720 **Fig. 4.** MS^2 spectra of ammoniated ($[M+NH_4]^+$) 1Hp-1G-BDGT (*m/z* 1687.5) and 1MeOG-1G-
721 AR (*m/z* 1078.9), respectively. The chemical structures and the formation of major product
722 ions are also drawn. The glycerol extension in the BDGT structure is either located at *sn*-1 or
723 *sn*-3 positions of the glycerol. Both, 1MeOG and 1Hp head group structures have only been
724 tentatively identified based on their exact mass in full scan and MS^2 experiments and their
725 full characterization requires further structural elucidation. However, for example for the peak

726 at *m/z* 1078.9 $[M+NH_4]^+$ we observed a dominant fragment ion associated with core Ext-AR
727 (62) in the MS^2 spectrum, resulting from a neutral loss of 1G + 176.1 Da + NH_3 and likely
728 indicating a methylated dihexose head group (96). We interpreted the spectrum to represent
729 a 1MeO-1G-Ext-AR. Similarly, we observed a loss of 2G + CH_2O + NH_3 (354.1 Da) and
730 BDGT core lipid fragment ions (37, 38) for the peak at *m/z* 1687.3 $[M+NH_4]^+$ and tentatively
731 identified this IPL as heptose-containing lipid, 1Hp-1G-BDGT. The polar head group is either
732 located at the glycerol or butanetriol moiety.

733 **Fig. 5.** (a) Magnified section of density map plot in the tetraether area showing the major
734 diagnostic ions of butanetriol and corresponding solely glycerol containing lipids in the TLE of
735 *M. luminyensis*, analyzed by RP-HPLC-MS. (b) and (c) show MS^2 spectra of sodiated
736 ($[M+Na]^+$) core BDGT (*m/z* 1338.3) and 1G-BDGT (*m/z* 1500.4), respectively. BDGT spectra
737 match those shown by Zhu et al. (37) and Knappy et al. (38). The glycerol extension in the
738 BDGT structure is either located at *sn*-1 or *sn*-3 positions of the glycerol and the polar head
739 group of intact BDGTs is either located at the glycerol or butanetriol moiety.

740 **Fig. 6.** (a) Relative abundance of different head groups in the TLE of *M. luminyensis*. (b)
741 Relative abundance of core lipids in the TLE, acid hydrolyzed TLE and acid hydrolyzed
742 biomass of *M. luminyensis*. For the TLE, free and head group-bound core lipids were
743 considered. For chemical structures and abbreviations see Fig. 2.

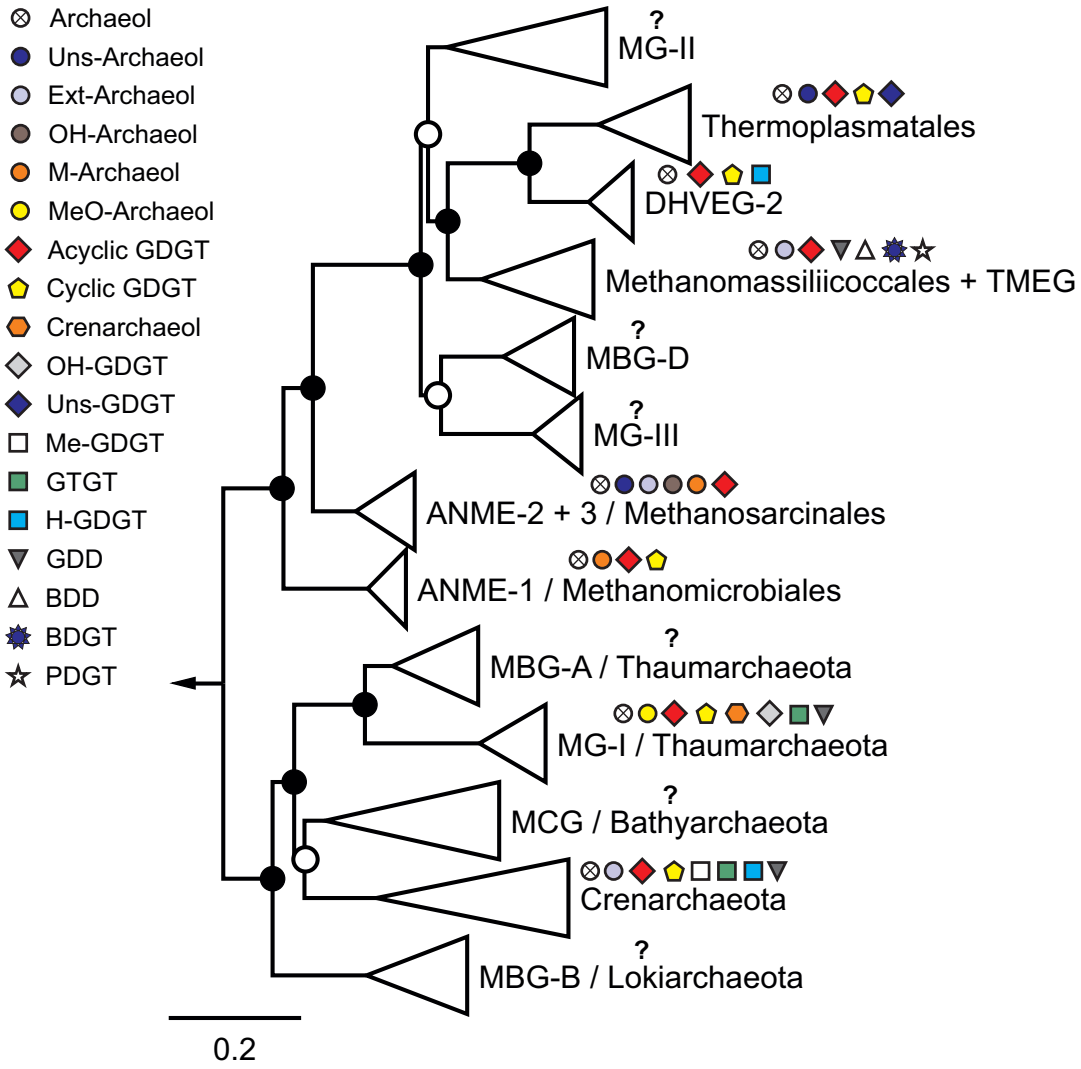
Archaeol
Uns-Archaeol
Ext-Archaeol
OH-Archaeol
M-Archaeol
MeO-Archaeol
Acyclic GDGT
Cyclic GDGT
Crenarchaeol
OH-GDGT
Uns-GDGT
Me-GDGT
GTGT
H-GDGT
GDD
BDD
BDGT
PDGT
?
MG-II
Thermoplasmatales
DHVEG-2
Methanomassiliicoccales + TMEG
?
MBG-D
?
MG-III
ANME-2 + 3 / Methanosarcinales
ANME-1 / Methanomicrobiales
?
MBG-A / Thaumarchaeota
MG-I / Thaumarchaeota
?
MCG / Bathyarchaeota
Crenarchaeota
?
MBG-B / Lokiarchaeota
0.2

Core lipids

Archaeol

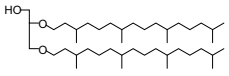

Extended archaeol

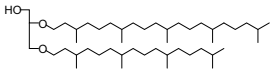

Diextended archaeol

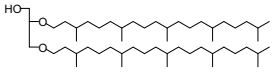

GDGT-0

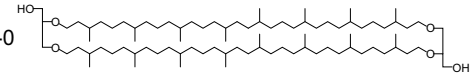

GDD-0

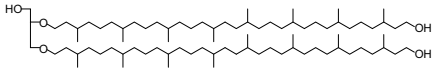

BDD-0

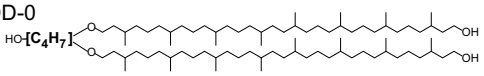

Polyprenols

BDGT-0

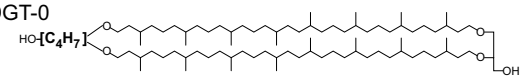

BDGT-1

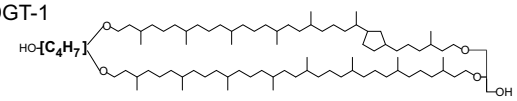

BDGT-2

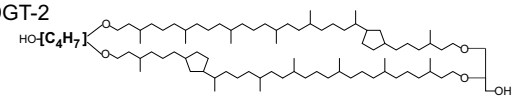

PDGT-0

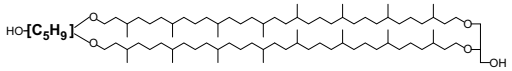

PDGT-1

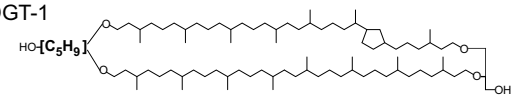

PDGT-2

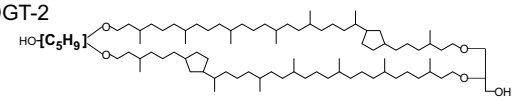

Head groups

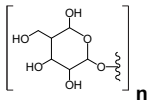

Monohexose (1G) n = 1
Dihexose (2G) n = 2
Trihexose (3G) n = 3

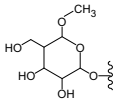

Methoxylated hexose (1MeOG)

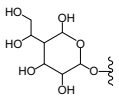

Heptose (1Hp)

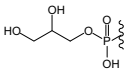

Phosphatidylglycerol (PG)

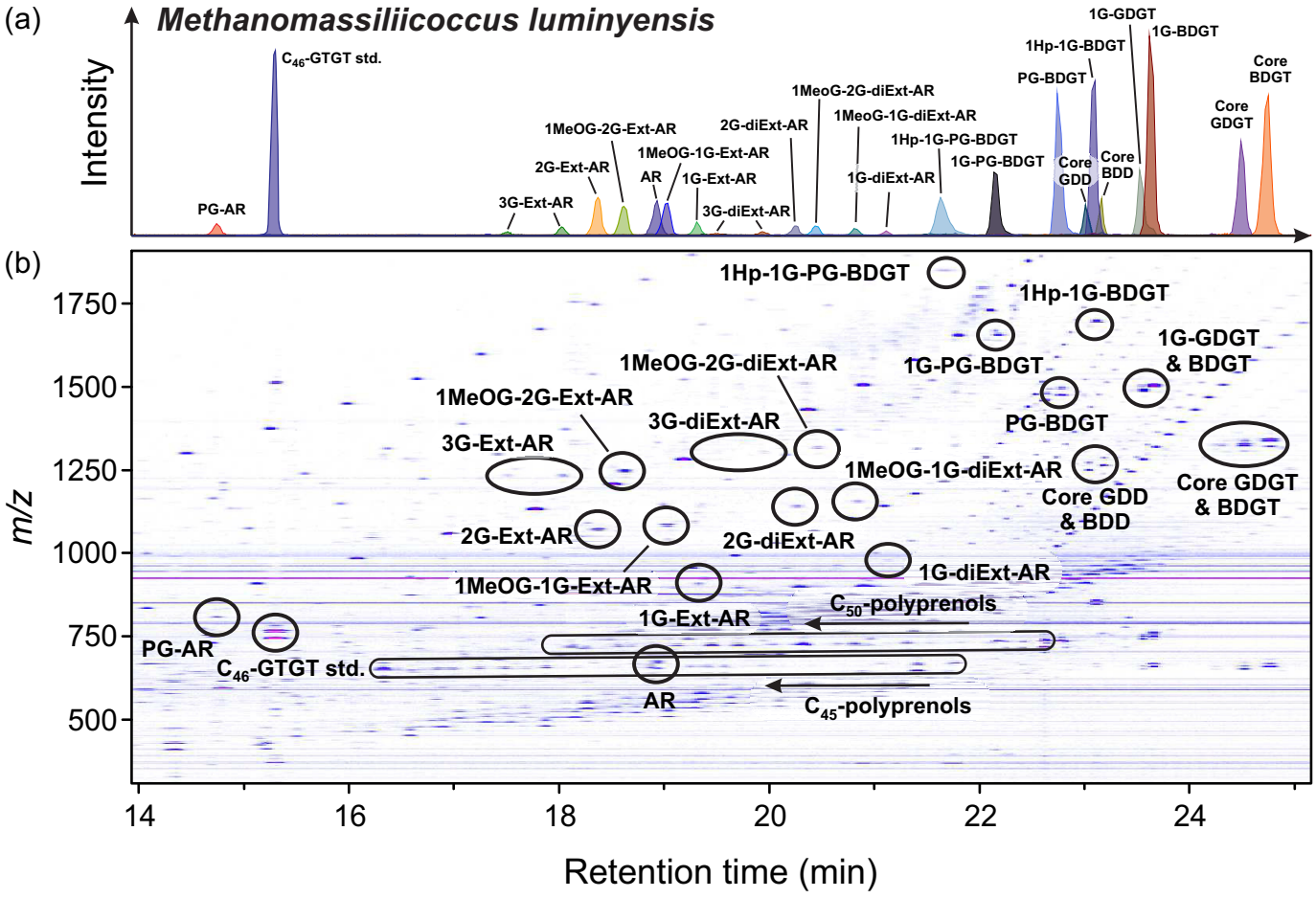
(a)
Methanomassiliicoccus luminyensis
Intensity
C46-GTGT std.
PG-AR
3G-Ext-AR
2G-Ext-AR
1MeOG-2G-Ext-AR
1MeOG-1G-Ext-AR
AR
1G-Ext-AR
2G-diExt-AR
3G-diExt-AR
1MeoG-2G-diExt-AR
1MeoG-1G-diExt-AR
1G-diExt-AR
1Hp-1G-PG-BDGT
1G-PG-BDGT
Core GDD
Core BDD
PG-BDGT
1Hp-1G-BDGT
1G-GDGT
1G-BDGT
Core GDGT
Core BDGT
(b)
m/z
1750
1500
1250
1000
750
500
14
16
18
20
22
24
Retention time (min)
1Hp-1G-PG-BDGT
1Hp-1G-BDGT
1G-GDGT & BDGT
1G-PG-BDGT
1MeOG-2G-diExt-AR
1MeOG-2G-Ext-AR
3G-diExt-AR
3G-Ext-AR
PG-BDGT
1MeOG-1G-diExt-AR
Core GDD & BDD
Core GDGT & BDGT
2G-Ext-AR
2G-diExt-AR
1G-diExt-AR
1MeOG-1G-Ext-AR
C50-polyprenols
1G-Ext-AR
PG-AR
C46-GTGT std.
AR
C45-polyprenols

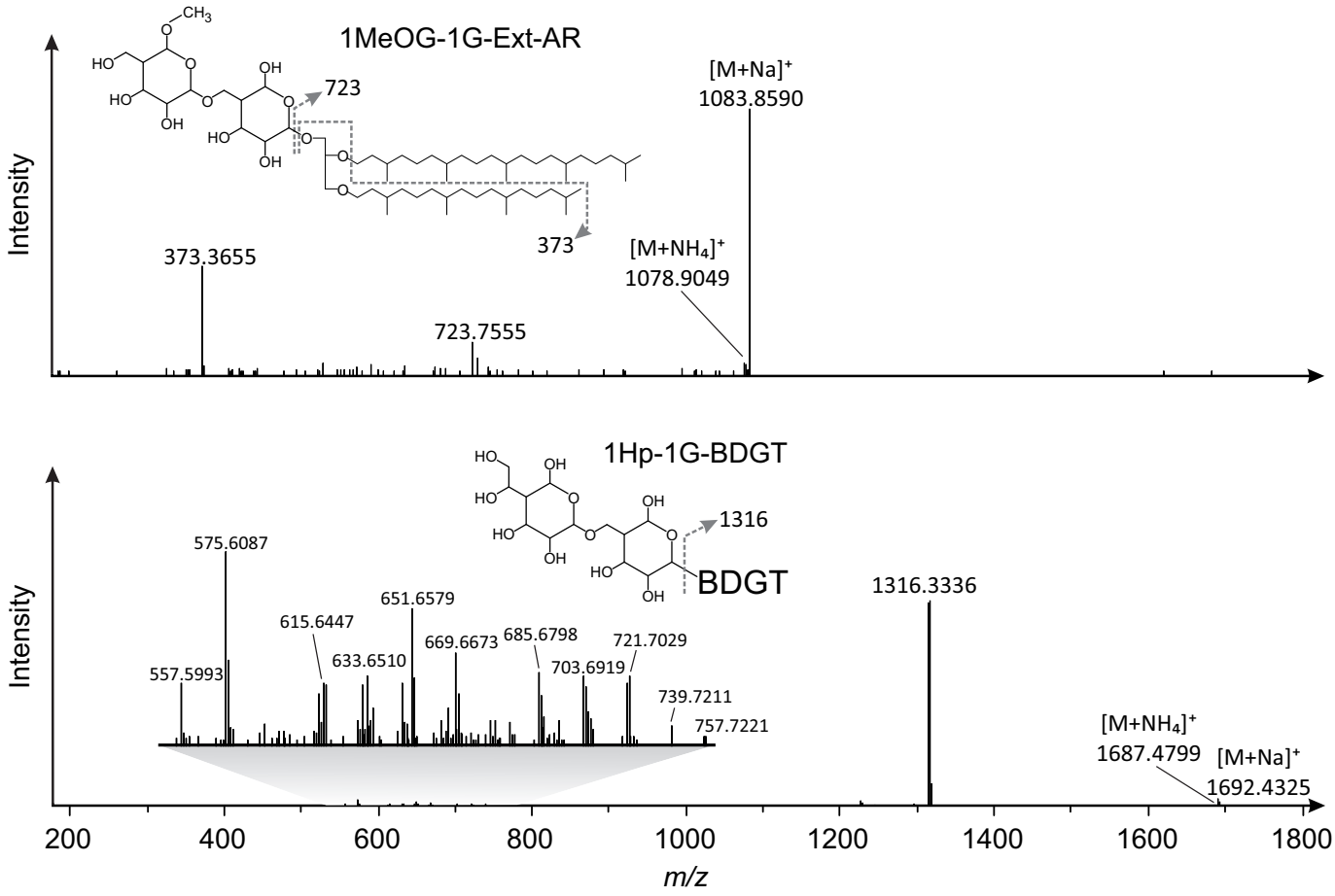
1MeOG-1G-Ext-AR
723
373
[M+Na]+
1083.8590
[M+NH4]+
1078.9049
373.3655
723.7555
Intensity
1Hp-1G-BDGT
1316
BDGT
575.6087
615.6447
651.6579
633.6510
669.6673
685.6798
721.7029
703.6919
557.5993
739.7211
757.7221
1316.3336
[M+NH4]+
1687.4799
[M+Na]+
1692.4325
Intensity
200
400
600
800
1000
1200
1400
1600
1800
m/z

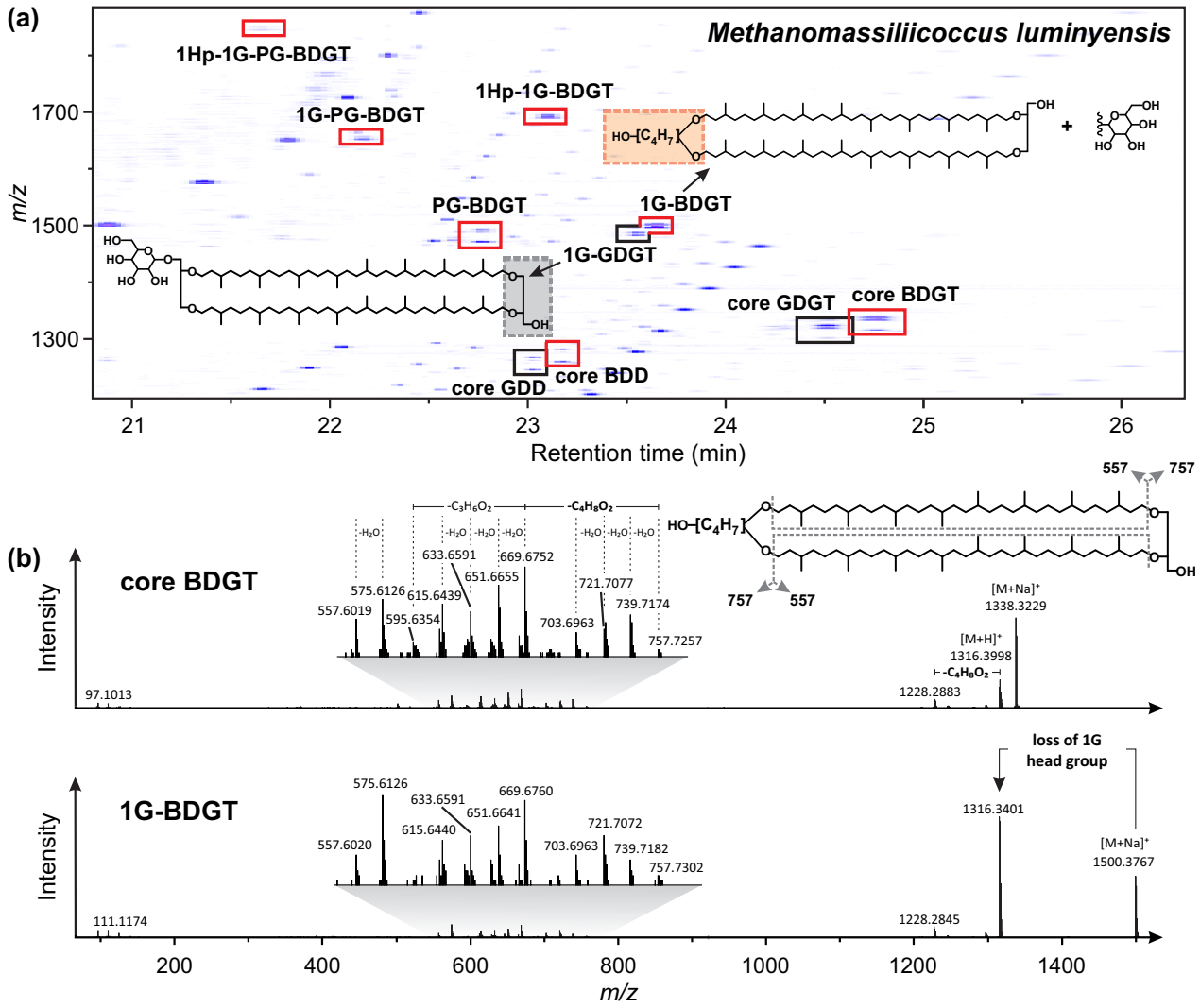
(a)
Methanomassiliicoccus luminyensis
1Hp-1G-PG-BDGT
1Hp-1G-BDGT
1G-PG-BDGT
PG-BDGT
1G-BDGT
1G-GDGT
core GDGT
core BDGT
core GDD
core BDD
m/z
Retention time (min)
(b)
core BDGT
Intensity
557
757
[M+Na]+
1338.3229
[M+H]+
1316.3998
1228.2883
97.1013
1G-BDGT
loss of 1G
head group
1316.3401
[M+Na]+
1500.3767
1228.2845
111.1174
m/z

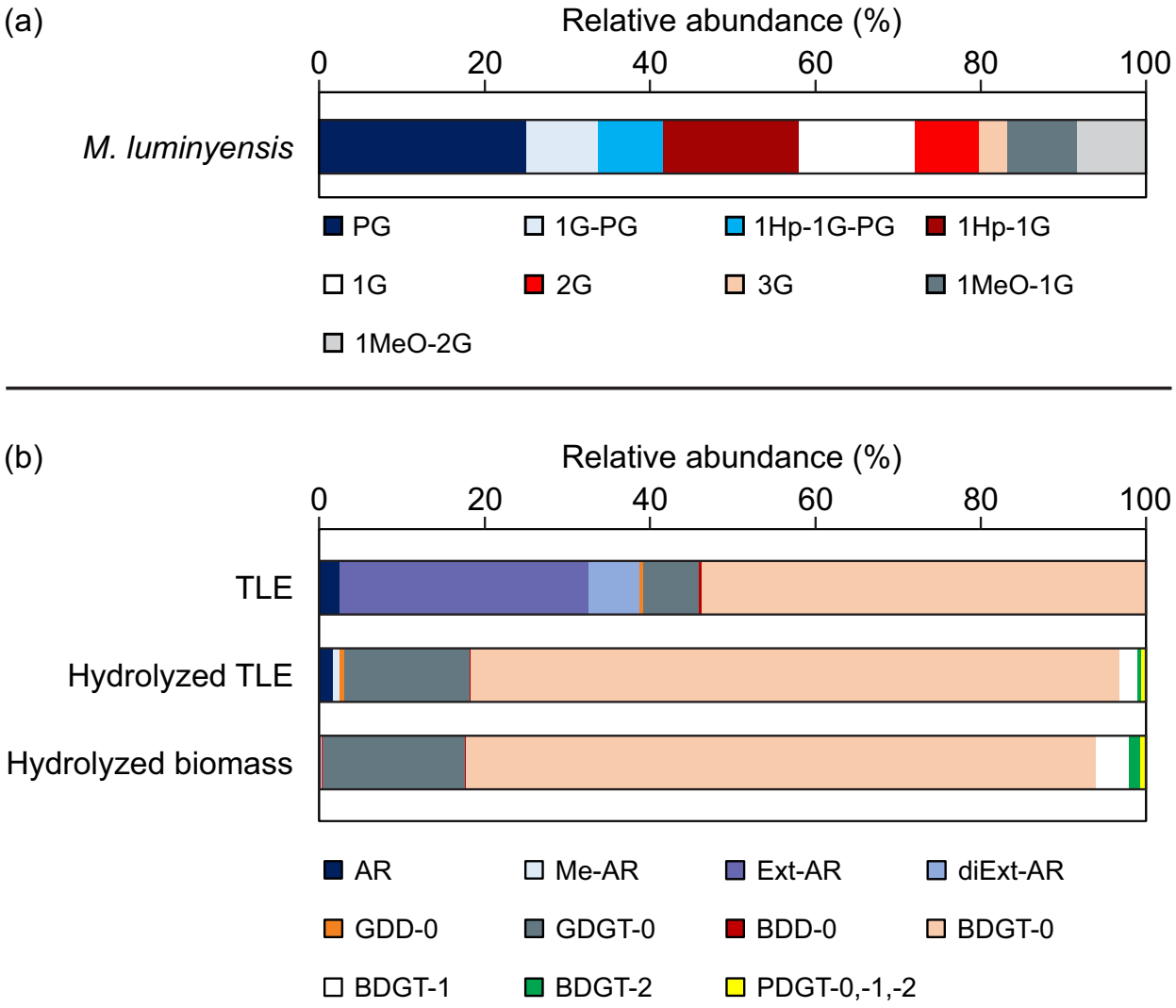
(a)
Relative abundance (%)
0
20
40
60
80
100
M. luminyensis
PG
1G-PG
1Hp-1G-PG
1Hp-1G
1G
2G
3G
1MeO-1G
1MeO-2G
(b)
Relative abundance (%)
0
20
40
60
80
100
TLE
Hydrolyzed TLE
Hydrolyzed biomass
AR
Me-AR
Ext-AR
diExt-AR
GDD-0
GDGT-0
BDD-0
BDGT-0
BDGT-1
BDGT-2
PDGT-0,-1,-2

Compound	*m/z* ($[M+H]^+$; $[M+NH_4]^+$; $[M+Na]^+$)	Characteristic fragment ions in MS^2	Retention time (min)	Relative lipid abundance (%)
GDD	1246.2965; 1263.3230; 1268.2784	669.7	23.0	0.3
BDD	1260.3121; 1277.3387; 1282.2940	683.7	23.2	0.3
GDGT	1302.3227; 1319.3492; 1324.3046	743.7	24.5	1.3
BDGT	1316.3383; 1333.3649; 1338.3203	757.7	24.8	2.1
1G-GDGT	1464.3755; 1481.4020; 1486.3574	1302.3; 743.7	23.5	3.0
1G-BDGT	1478.3911; 1495.4177; 1500.3731	1316.3; 757.7	23.6	6.7
PG-BDGT	1470.3414; 1487.3680; 1492.3234	a)	22.8	19.0
1G-PG-BDGT	1632.3943; 1649.4208; 1654.3762	1470.3	22.2	6.8
1Hp-1G-BDGT	1670.4545; 1687.4811; 1692.4365	1316.3	23.1	13.1
1Hp-1G-PG-BDGT	1824.4576; 1841.4842; 1846.4396	b)	21.6	6.2
AR	653.6806; 670.7072; 675.6626	373.4	19.0	0.8
PG-AR	807.6837; 824.7103; 829.6657	733.6; 537.4	14.8	0.8
1G-Ext-AR	885.8117; 902.8382; 907.7936	373.4; 443.5; 723.8	19.3	1.1
1G-diExt-AR	955.8899; 972.9165; 977.8719	443.5; 793.8	21.1	0.4
1MeOG-1G-Ext-AR	1061.8802; 1078.9067; 1083.8621	373.4; 443.5; 723.8	19.0	5.5
2G-Ext-AR	1047.8645; 1064.8911; 1069.8465	373.4; 443.5; 723.8	18.4	6.1
1MeOG-1G-diExt-AR	1131.9584; 1148.9850; 1153.9404	443.5; 793.8	20.8	1.3
2G-diExt-AR	1117.9428; 1134.9693; 1139.9247	443.5; 793.8	20.3	1.7
1MeOG-2G-Ext-AR	1223.9330; 1240.9595; 1245.9149	373.4; 443.5; 723.8	18.6	4.9
3G-Ext-AR (a)	1209.9173; 1226.9439; 1231.8993	373.4; 443.5; 723.8	17.5	0.6
3G-Ext-AR (b)	1209.9173; 1226.9439; 1231.8993	373.4; 443.5; 723.8	18.0	1.4
1MeOG-2G-diExt-AR	1294.0112; 1311.0378; 1315.9932	443.5; 793.8	20.5	1.6
3G-diExt-AR (a)	1279.9956; 1297.0221; 1301.9775	443.5; 793.8	19.5	0.3
3G-diExt-AR (b)	1279.9956; 1297.0221; 1301.9775	443.5; 793.8	20.0	0.5
$C_{50:1}$ - $C_{50:10}$ polyprenols	699.6-717.8; 716.7-734.8; 721.6-739.8	loss of H_2O (-18.0 Da)	18.1-22.6	8.5
$C_{45:0}$ - $C_{45:9}$ polyprenols	631.6-649.7; 648.6- 666.7; 653.6-671.7	loss of H_2O (-18.0 Da)	16.4-21.7	5.6

a) fragmentation not fully resolved

b) no MS^2 data available

Cruise	Site and Core	Sediment depth (m)	Total organic carbon (wt%)	% BDGTs
M76/1	GeoB12806-2	0.1	8.9	n.d.
(Namibia Margin)	GeoB12807-2	3.1	7.4	0.21
ODP201	1229D 4H4	30.7	4.7	0.36
(Peru Margin)	1229A 22H1	185.9	0.47	3.5
ODP201	1226B 10H3	83.8	1.1	n.d.
(Equatorial Pacific)	1226E 20H3	320	0.28	n.d.
ODP204	1250D 6H5	43.5	0.96	1.1
(Hydrate Ridge)	1250D 12H5	100.3	1.3	0.12
IODP311	1237C 10H5	79.8	0.64	n.d.
(Cascadia Margin)	1237C 13C6	109.8	0.56	0.21
ODP 160	966C 5H02	40	5.7	0.81
(Mediterranean Sapropel)	966C 7H04	65	7.4	0.34